

# Infrared Brazing of $\text{Ti}_{50}\text{Ni}_{50}$ Shape Memory Alloy Using Gold-based Braze Alloys

**RH Shiue and SK Wu\***

Department of Materials Science and Engineering,  
National Taiwan University, Taipei 106, Taiwan

\*Corresponding author

Prof. Shyi-Kaan Wu

E-mail: skw@ntu.edu.tw

Tel: + 886-2-2363-7846

Fax: + 886-2-2363-4562

## Abstract

**Infrared brazing  $\text{Ti}_{50}\text{Ni}_{50}$  shape memory alloy using pure Au and Au-20Cu as the fillers has been investigated. The Au-rich and  $\text{Au}_4\text{Ti}$  phases, and  $\text{Au}_2\text{TiNi}$ , AuCu and  $\text{Ni}_3\text{Ti}$  phases are formed in the brazed joints using Au filler and Au-20Cu filler, respectively. The bending test shows the shape memory effect of brazed joint using Au filler is superior to that using Au-20Cu filler because the detrimental AuCu and  $\text{Ni}_3\text{Ti}$  phases exist in the latter case.**

## Keywords

1. brazing; 2. SEM; 3.  $\text{Ti}_{50}\text{Ni}_{50}$  shape memory alloy;  
4. interfaces

## Introduction

$\text{Ti}_{50}\text{Ni}_{50}$  shape memory alloy (SMA) which exhibits a strong shape memory effect has been considered as a good candidate for aerospace or medical applications (1-3). The development of joining process is always important in the application of many engineering alloys.  $\text{Ti}_{50}\text{Ni}_{50}$  SMA can be joined by brazing without melting the base metal in order to keep its shape memory effect as well as mechanical properties (4). Compared with the traditional furnace brazing, infrared brazing is suitable in studying the microstructural evolution of the joint with the advantage of its rapid heating rate as high as 3000°C per minute. Additionally, the brazing cycle does less damage to the base metal during infrared brazing (5,6).

The selection of filler metal plays a key role in brazing  $\text{Ti}_{50}\text{Ni}_{50}$  SMA. The wettability of the molten braze on  $\text{Ti}_{50}\text{Ni}_{50}$  substrate, the shape memory effect of the brazed joint and the formation of intermetallic phases in the joint should be considered together in choosing the filler metal. It has been reported that replacing Ni in the  $\text{Ti}_{50}\text{Ni}_{50}$  SMA by Au or Cu to form  $\text{Ti}_{50}\text{Ni}_{50-x}\text{Au}_x$  or  $\text{Ti}_{50}\text{Ni}_{50-x}\text{Cu}_x$  alloys can still preserve its shape memory effect (7,8). Based on previous studies,  $\text{Ti}_{50}\text{Ni}_{50}$  can be infrared brazed using pure Cu as the filler metal, and the Ti(Ni,Cu) phase in the brazed joint exhibits the shape memory behavior even it has alloyed with a huge amount of Cu (4). Since Au and Cu is completely miscible above 410°C, it should be possible to infrared braze  $\text{Ti}_{50}\text{Ni}_{50}$  SMA using Au-Cu alloys without detrimental effect to its shape memory effect. The melting point of pure Au is 1064.4°C. The Au-20Cu alloy in weight percent has the lowest liquidus temperature of 910°C in the Au-Cu binary alloy system (9). Therefore, these compositions have been chosen as braze alloys in this study. The purpose of this investigation is focused on the microstructural evolution and shape memory behaviour of the infrared brazed  $\text{Ti}_{50}\text{Ni}_{50}$  joints. The feasibility of infrared brazing  $\text{Ti}_{50}\text{Ni}_{50}$  alloy using Au and Au-20Cu as the braze alloys is also evaluated.

## Experimental procedure

$\text{Ti}_{50}\text{Ni}_{50}$  SMA was prepared by vacuum arc remelting (VAR) of titanium rods (purity: 99.7wt%) and nickel pellets (purity: 99.9wt%). Both titanium rods and nickel pellets were cleaned by 1HF-15HNO<sub>3</sub>-64H<sub>2</sub>O (in ml) and saturated NaOH solution prior to performing VAR. Foils of Au-20Cu in weight percent and pure Au foils (purity : 99.99wt%) were selected as braze alloys, and their thickness was kept at 70μm throughout the experiments.

The infrared furnace used in this study was ULVAC SINKO-RIKO RHL-P610C with the maximum heating rate of about 3000°C/min (10). Infrared brazing was performed under the vacuum of  $5 \times 10^{-5}$  mbar, and the heating rate was set at 900°C/min. All specimens were preheated at 600°C for 60 sec to equilibrate the actual temperature in the specimen.

The process variables used in the experiments are listed in Table 1.

The size of brazed specimens was 10.0x10.0x2.5 mm<sup>3</sup>. All mating surfaces were polished by SiC paper to grit 600 and ultrasonically cleaned in acetone before infrared brazing. The area of the filler foils was approximately the same as that of the base metal. A graphite fixture was used in order to enhance the absorption of infrared radiation during infrared brazing. Specimens were sandwiched between two graphite plates, and an R-type thermocouple in the upper graphite plate was contacted with the specimen.

The cross-sections of the brazed joints were examined by using a Philips XL-30 scanning electron microscope (SEM) equipped with an energy dispersive spectrometer (EDS). Quantitative chemical analyses were performed by using a JEOL JXA 8600SX electron probe microanalyzer (EPMA) equipped with a wavelength dispersive spectrometer (WDS). The operation voltage was 20 kV and its spot size was about 1µm.

The shape memory effect was evaluated by bending test as illustrated in Fig. 1. The shape recovery ratio of infrared brazed joint was obtained from the bending test (4,11). The dimension of the samples used in the bending test was 60.0x5.0x0.5 mm<sup>3</sup>. The specimen was initially bent to  $\theta_i$  in the liquid nitrogen (77K). Next, the specimen's temperature was increased to 403K to measure the shape recovery angle ( $\theta_f$ ). The shape recovery ratio of the brazed joint was defined by the following equation (4,11):

$$\text{Shape recovery ratio} = (\theta_i - \theta_f) / \theta_i \times 100\%$$

Additionally, the shape recovery ratio of Ti<sub>50</sub>Ni<sub>50</sub> substrate with the identical dimension was also performed for the purpose of comparison.

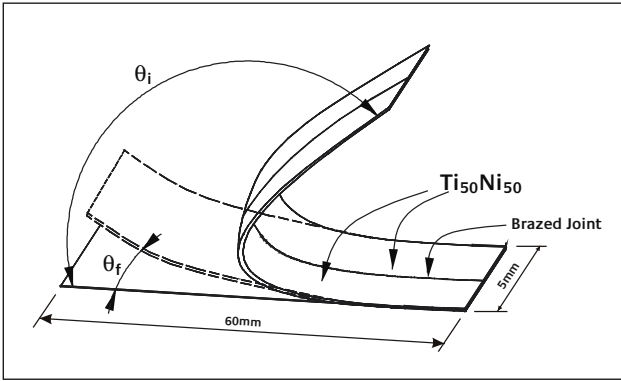


**Figure 1**  
The schematic diagram of bending test specimen to measure the shape recovery ratio (8)

**Table 1**  
Summary of process variables used in this study

Braze Alloy	Brazing Temperature (°C)	Brazing Time (seconds)			
Au-20Cu	950	15 <sup>M</sup>	60 <sup>M</sup>	180 <sup>M</sup>	300 <sup>M</sup>
	980	15 <sup>M</sup>	60 <sup>M, B</sup>	180 <sup>M, B</sup>	300 <sup>M</sup>
	1010	15 <sup>M</sup>	60 <sup>M, B</sup>	180 <sup>M, B</sup>	300 <sup>M</sup>
Au	1100	15 <sup>M</sup>	60 <sup>M, B</sup>	180 <sup>M, B</sup>	300 <sup>M</sup>

M: metallurgical observation specimen, B: bending test specimen

## Results and discussion

### Infrared brazed joint of Ti<sub>50</sub>Ni<sub>50</sub> SMA with Au-20Cu braze alloy

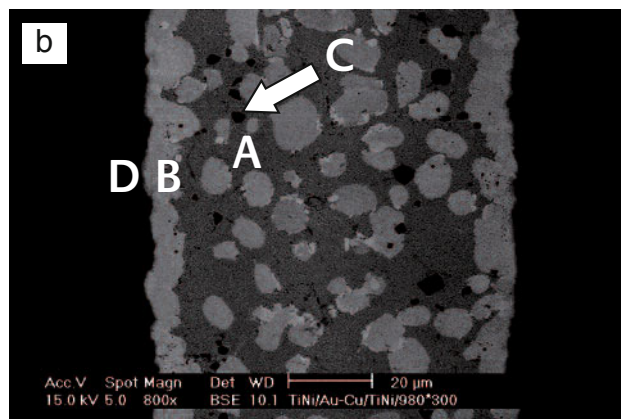
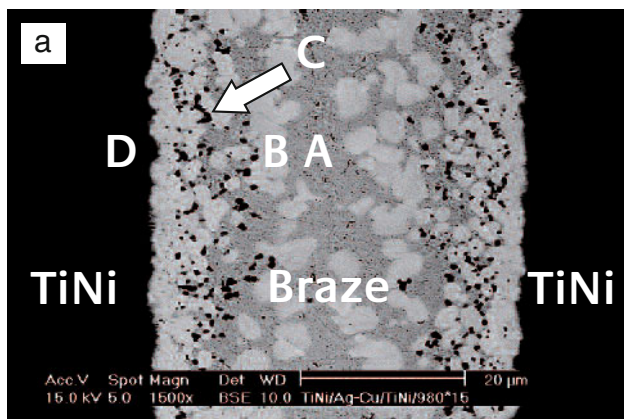
Figures 2(a) and 2(b) show the SEM backscattered electron images (BEIs) and EPMA chemical analysis results of Ti<sub>50</sub>Ni<sub>50</sub>/Au-20Cu/Ti<sub>50</sub>Ni<sub>50</sub> specimen infrared brazed at 980°C for 15 and 300 seconds, respectively. Based on the EPMA results, there are at least three phases readily observed in the brazed joint, including AuCu, Au<sub>2</sub>NiTi and Ni<sub>3</sub>Ti phases as marked by A, B and C in Figure 2. The infrared brazed joint mainly consists of AuCu and Au<sub>2</sub>NiTi phases. The dissolution of Ti<sub>50</sub>Ni<sub>50</sub> substrate into the molten braze causes reactions among Ti, Ni, Au and Cu. Therefore, Au<sub>2</sub>NiTi and black globular Ni<sub>3</sub>Ti precipitates are formed in the joint. The Ni<sub>3</sub>Ti phase is greatly coarsened as the brazing time increased from 15s to 300s. It is also noted that the formation of interfacial Ti(Ni,Au) phase as marked by D in the figure results from Au dissolved in the Ti<sub>50</sub>Ni<sub>50</sub> substrate. However, Cu is absent from the Ti<sub>50</sub>Ni<sub>50</sub> substrate and its surface.

Figure 3 displays the SEM BEI result of the infrared brazed Ti<sub>50</sub>Ni<sub>50</sub>/Au-20Cu/Ti<sub>50</sub>Ni<sub>50</sub> specimen at 980°C for 60s at higher magnification. It is important to note that there is a fine lamellar shape interfacial layer formed between the braze and Ti<sub>50</sub>Ni<sub>50</sub> substrate. The chemical composition of area marked E in atomic percent is 7.3% Cu, 28.6% Ti, 60.0% Ni and 4.1% Au, which is close to (Au,Cu,Ni)<sub>3</sub>Ti. The composition of the lamellar structure cannot be accurately determined due to the limited lateral resolution of EPMA, and it needs further study.

Figures 4 shows the SEM BEI of Ti<sub>50</sub>Ni<sub>50</sub>/Au-20Cu/Ti<sub>50</sub>Ni<sub>50</sub> specimen infrared brazed at 1010°C for 300 seconds. The higher brazing temperature accelerates the microstructural evolution of the brazed joint. The amount of Au<sub>2</sub>NiTi phase increases while that of AuCu phase decreases in the braze. However, the black globular Ni<sub>3</sub>Ti phase significantly decreases due to the consumption of Ni and Ti in forming Au<sub>2</sub>NiTi phase.

### Infrared brazed joint of Ti<sub>50</sub>Ni<sub>50</sub> SMA with Au braze alloy

The melting temperature of Au is 1064.4°C, so the selection of 1100°C brazing temperature is practical to braze the Ti<sub>50</sub>Ni<sub>50</sub> SMA by using the pure Au filler. Figures 5(a) and 5(b) show the SEM BEIs and EMPA chemical analysis results of Ti<sub>50</sub>Ni<sub>50</sub>/Au/Ti<sub>50</sub>Ni<sub>50</sub> specimen infrared brazed at 1100°C for



Element (at%)	A	B	C	D	A	B	C	D
	(a) After 15s at 980°C				(b) After 300s at 980°C			
Cu	45.5	4.2	---	---	54.2	---	---	---
Ti	4.8	25.7	24.1	48.3	4.2	25.8	25.1	49.1
Ni	4.8	20.8	74.8	50.3	8.9	23.6	73.0	47.9
Au	44.9	49.3	1.1	1.4	32.7	50.6	1.9	3.0
Possible phase	AuCu	Au <sub>2</sub> NiTi	Ni <sub>3</sub> Ti	Ti(Ni,Au)	AuCu	Au <sub>2</sub> NiTi	Ni <sub>3</sub> Ti	Ti(Ni,Au)

**Figure 2**

SEM BEIs and EPMA chemical analysis results of  $Ti_{50}Ni_{50}/Au-20Cu/Ti_{50}Ni_{50}$  specimens infrared brazed at 980°C for (a) 15s, (b) 300s

15 and 300 seconds, respectively. Based on the EPMA results, the infrared brazed joint primarily consists of the Au-rich phases alloyed with different amount of Ti and Ni. The white Au-rich phase has lower content of Ti as illustrated by A in Figure 5. The grey Au-rich phase contains higher content of Ti as marked by B in Figure 5. Unfortunately, the Au-Ni-Ti ternary alloy phase diagram is unavailable in the literature. According to the binary phase diagram of Au-Ti, the highest solubility of Ti in Au is 12 at% at 1123°C (9). In contrast, the solubility of Au in Ti is less than 2 at% at room temperature. Consequently, the formation of two Au-rich phases is primarily caused by the limited solubility of Ti in the Au-rich alloy.

According to the binary Au-Ti phase diagram, there is a peritectic reaction at 1123°C,  $(Au) \leftrightarrow L + Au_4Ti$  (9). Although the brazing temperature (1100°C) is below 1123°C, the  $Au_4Ti$

phase is also possibly formed via interfacial reaction as well as interdiffusion. Based on the experimental observation, there is a reaction layer at the interface between the braze and  $Ti_{50}Ni_{50}$  substrate as marked by C in Figure 5. The stoichiometric ratio between  $(Au+Ni)$  and Ti is close to 4, so  $(Au,Ni)_4Ti$  is the most possible interfacial phase.

Similar to the result for Au-20Ni, the Au filler foil is partly dissolved into the  $Ti_{50}Ni_{50}$  substrate, as shown in D in Figure 5. The alloying of Au into the  $Ti_{50}Ni_{50}$  base metal results in Ni replaced partially by Au to form the  $Ti(Ni,Au)$  at the substrate close to infrared brazed joint. There is no significant change of reaction phases in the brazed joint, however, the amount of grey Au-rich phase significantly increases as the brazing time increases from 15s to 300s due to the higher dissolution of  $Ti_{50}Ni_{50}$  substrate into the molten braze during brazing.

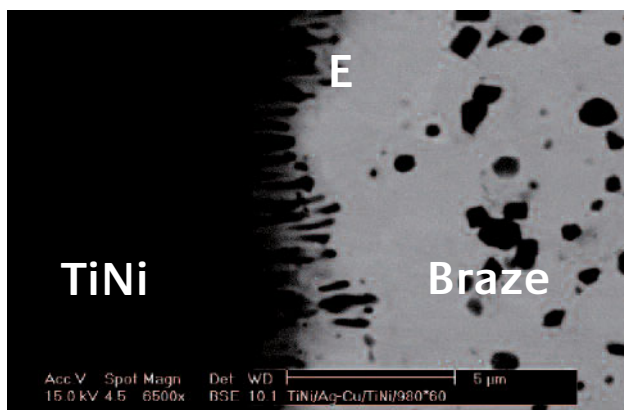


**Figure 3**

The SEM BEI result of  $Ti_{50}Ni_{50}/Au-20Cu/Ti_{50}Ni_{50}$  specimen infrared brazed at 980°C for 60s at higher magnification

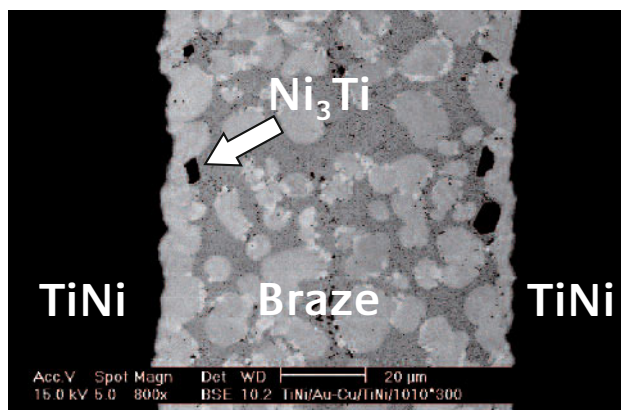
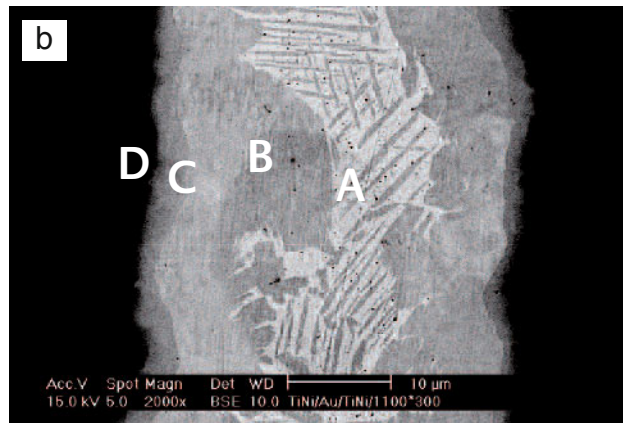
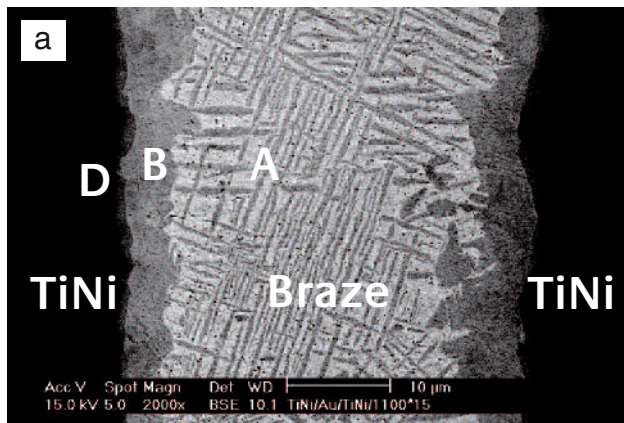


**Figure 4**

The SEM BEI result of  $Ti_{50}Ni_{50}/Au-20Cu/Ti_{50}Ni_{50}$  specimen infrared brazed at 1010°C for 300s





Element (at%)	A	B	C	D	A	B	C	D
Ti	4.3	11.0	22.7	49.8	2.5	11.9	20.8	46.4
Ni	8.1	8.8	4.8	46.1	7.3	6.7	5.6	43.2
Au	87.6	80.2	72.5	4.1	90.2	81.4	73.6	10.4
Possible phase	Au-rich	Au-rich	Au <sub>4</sub> Ti	Ti(Ni,Au)	Au-rich	Au-rich	Au <sub>4</sub> Ti	Ti(Ni,Au)

**Figure 5**

SEM BEIs and EPMA chemical analysis results of  $Ti_{50}Ni_{50}/Au/Ti_{50}Ni_{50}$  specimens infrared brazed at 1100°C for (a) 15s, (b) 300s

### Shape recovery tests of infrared brazed

#### $Ti_{50}Ni_{50}$ alloy

Table 2 summarizes the shape recovery ratios of  $Ti_{50}Ni_{50}$  base metal and infrared brazed joints using Au-20Cu and Au fillers with various brazing conditions. The experiment results indicate the shape recovery effect of infrared brazed  $Ti_{50}Ni_{50}$  using Au filler alloy is much better than that using Au-20Cu braze alloy. The shape recovery ratio of the infrared brazed joint using Au filler is identical to that of the  $Ti_{50}Ni_{50}$  base metal. The pure gold brazed joint demonstrates excellent ductility, and there is no crack on the brazed joint after bending test. Accordingly, the Au-rich phases in the joint are not detrimental to the shape memory effect of infrared brazed  $Ti_{50}Ni_{50}$  SMA.

The shape recovery ratios of the infrared brazed joints using Au-20Cu filler are much lower than those of Au brazed joints. The cross-section of the bending test specimen was cut and mounted in an epoxy resin for SEM inspection. Figure 6 shows the SEM images of the bent specimen infrared brazed at 980°C and 180s with Au-20Cu braze alloy.

**Table 2**

Shape recovery ratios of  $Ti_{50}Ni_{50}$  base metal and infrared brazed joints using Au-20Cu and Au fillers

Specimen	Shape Recovery Ratio
Au-20Cu foil at 980°C for 60s	64%
Au-20Cu foil at 980°C for 180s	68%
Au foil at 1100°C for 60s	> 99%
Au foil at 1100°C for 180s	> 99%
$Ti_{50}Ni_{50}$ Base Metal	> 99%

There are large holes in the joint as indicated by arrows in Figure 6(b). These pores are initiated in the AuCu matrix close to the  $Ni_3Ti$  phase, so the presence of both AuCu and  $Ni_3Ti$  phases does damage to the shape memory effect of the infrared brazed  $Ti_{50}Ni_{50}$  alloy. Additionally, the AuCu phase cannot be completely removed from the joint by the optimization of the brazing process variables.

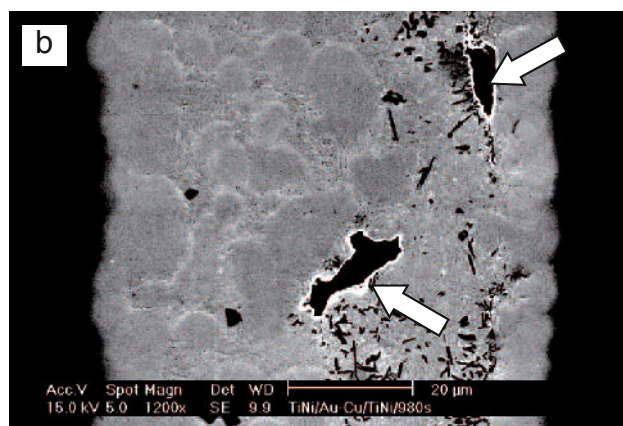
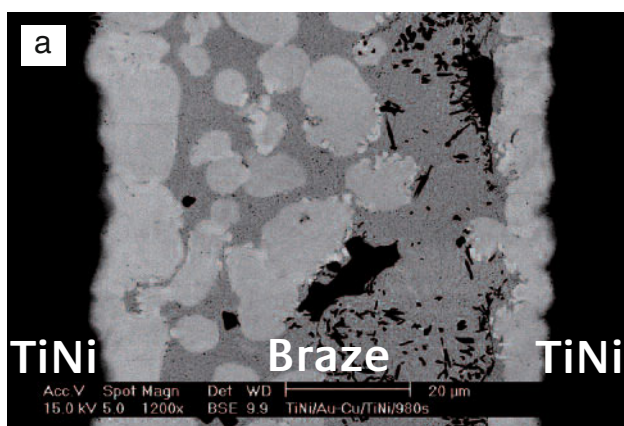


**Figure 6**

SEM images of the bent specimen infrared brazed at 980°C and 180s with Au-20Cu braze alloy: (a) BEI, (b) SEI

## Conclusions

Microstructural evolution, interfacial reaction and shape recovery behavior of infrared brazed  $\text{Ti}_{50}\text{Ni}_{50}$  shape memory alloy using Au-20Cu and Au fillers have been studied. The infrared brazed joint using Au-20Cu filler mainly comprises  $\text{Au}_2\text{NiTi}$ ,  $\text{AuCu}$  and  $\text{Ni}_3\text{Ti}$  intermetallics. The existence of these intermetallic phases degrades the shape recovery ratio of the infrared brazed joint. In contrast, the infrared brazed joint using the pure Au filler consists of huge amount Au-rich phase in the brazement and  $\text{Au}_4\text{Ti}$  reaction layer at the interface between the braze alloy and  $\text{Ti}_{50}\text{Ni}_{50}$ . Additionally, the  $\text{Ti}_{50}\text{Ni}_{50}$  substrate close to the infrared brazed joint is minor alloyed with Au and forms the  $\text{Ti}(\text{Ni},\text{Au})$  phase. The shape recovery ratio of the infrared brazed joint using Au filler is identical to that of  $\text{Ti}_{50}\text{Ni}_{50}$  base metal, and there is no crack in the brazed joint after bending test. Accordingly, the Au-rich phase in the joint is not detrimental to the shape memory effect of infrared brazed  $\text{Ti}_{50}\text{Ni}_{50}$  SMA. The pure Au filler metal demonstrates the potential application in brazing  $\text{Ti}_{50}\text{Ni}_{50}$  shape memory alloy.

## Acknowledgements

The authors gratefully acknowledge the financial support of this study from National Science Council (NSC), Republic of China, under the Grant of NSC 94-2216-E002-013.

## References

- 1 S. Miyazaki, K. Otsuka, Y. Suzuki, *Scripta Metall.*, 1981, **287**, 15
- 2 P. Filip, J. Lausmaa, J. Musialek, K. Mazanec, *Biomaterials*, 2001, **2131**, 22.
- 3 H.C. Lin, S.K. Wu, *Scripta Metall. Mater.*, 1992, **59**, 26
- 4 T.Y. Yang, R.K. Shiue, S.K. Wu, *Intermetallics*, 2004, **1285**, 12
- 5 R.K. Shiue, S.K. Wu, S.Y. Chen, *Acta Mater.* 2003, **1991**, 51
- 6 R.K. Shiue, S.K. Wu, C.H. Chan, *J. Alloy Comp.*, 2004, **148**, 372
- 7 O. Mercier, K.N. Melton, *Metall. Trans.*, 1979, **10A**, 387
- 8 S.K. Wu, C.M. Wayman, *Metallography*, 1987, **20**, 359
- 9 T.B. Massalski, Binary Alloy Phase Diagrams, ASM Int., Ohio, 1990
- 10 R.K. Shiue, S.K. Wu, C.H. Chan, *Metall. Mater. Trans.*, 2004, **35A**, 3177
- 11 H.C. Lin, S.K. Wu, *Scripta Metall. Mater.*, 1992, **59**, 26